Investigation of effects of energy-level degeneracy in cooperative Raman scattering of light

A. A. Zabolotskiĭ, S. G. Rautian, V. P. Safonov, and B. M. Chernobrod

Institute of Automation and Electronics, Siberian Division, USSR Academy of Sciences

The role of energy-level degeneracy in the cooperative Raman scattering (CRS) of light is investigated experimentally and theoretically. A radical difference is observed between the pulse shapes of rotational CRS in para- and orthohydrogen. Pulsations of the scattering intensity are observed in the model with two-level scattering in parahydrogen (transition $J_1 = 1$, $M_1 = 0 \rightarrow J_2 = 2$, $M_2 = 2$). The CRS pulse has a smooth envelope in the case of scattering in orthohydrogen, when three pairs of magnetic sublevels combine ($J_1 = 1$, $M_1 = 1, 0, -1 \rightarrow J_2 = 3$, $M_2 = 3, 2, 1$). A theoretical analysis has shown that the observed difference in the pulse shapes is due to nonsynchronous transitions of the molecules in different sublevel pairs in the case of orthohydrogen. The results of the numerical calculation agree qualitatively with the experimental data.

1. INTRODUCTION

In cooperative radiative processes, the molecules interact effectively via the radiation field and induce one another to emit energy more rapidly than in the case of an individual emitter. This produces in the medium a coherent light pulse having a duration much shorter than the time of the spontaneous radiation of an individual emitter. The theory of such processes is simplest in the case when the size of the volume occupied by the molecules is much smaller than the wavelength. Experiments in the optical region, however, involve volumes much larger than the wavelength. It became therefore clear even after the first experimental study[1] that propagation effects play an important role. In the simplest one-dimensional model allowance for propagation leads to a temporal substructure of the emission pulse.[2] This conclusion of the theory was in qualitative but not quantitative agreement with the experimental results. In particular, according to the one-dimensional theory the intensity drops to zero between the individual spikes, whereas only a weak modulation was observed in experiment and could vanish when the experimental conditions were changed.[3] This discrepancy between theory and experiment was observed both in emission[1,3] and in scattering.[4,5]

The finite transverse dimensions of the medium were taken into account in a number of recent experiments.[6,7] The transverse inhomogeneity caused a partial blurring of the temporal structure. A theory that claims quantitative agreement with experiment must therefore make allowance for the tranverse inhomogeneity of the medium and for diffraction effects. Investigations of cooperative radiative processes have thus become highly detailed.

The role played by degeneracy of the energy levels in the formation of the cooperative-radiation pulse has so far hardly been investigated. It was stated in Ref. 2 that level degeneracy does not alter qualitatively the character of a cooperative process. In Ref. 8, however, was reported observation of substantially different waveforms of the cooperative rotational Raman scattering pulses in para- and orthohydrogen. Whereas in the former case the scattering pulse shape had the characteristic temporal structure of cooperative scattering in a nondegenerate system, there was no temporal structure for scattering by orthohydrogen. This difference was attributed to level degeneracy. In the case of parahydrogen the combining levels are characterized by angular momenta $J_1 = 0$ and $J_2 = 2$. If the exciting field is circularly polarized the transition is only between two magnetic sublevels $J_1 = 0$, $M_1 = 0$ and $J_2 = 2$, $J_2 = 2$ (Fig. 1a). In scattering by orthohydrogen, transitions occurred between three pairs of sublevels $J_1 = 1$, $M_1 = -1, 0, 1$ and $J_2 = 3$, $M_2 = 1, 2, 3$ (Fig. 1b). The characteristic times of the molecule transitions between the corresponding sublevels depend on the values of the matrix elements of the interaction operator; they are different for the indicated sublevel pairs, so that the kinetics of the transitions between these sublevel pairs should be different. This desynchronization of the transitions can influence substantially the shape of the cooperative emission and scattering pulse.

The present paper is devoted to an experimental and theoretical investigation of the role of level degeneracy in cooperative Raman scattering (CRS). We investigate, in particular, scattering in para- and orthohydrogen and compare the results with the theory. It is remarkable that in rotational CRS in parahydrogen there is realized a model situation of scattering with sublevels combining into only one spectral component. The point is that in rotational forward RS the scattering cross section is a maximum when the circular polarizations of the exciting and Stokes fields are oppositely directed,[9] so that no parametric onset of an anti-Stokes component is possible.[10]
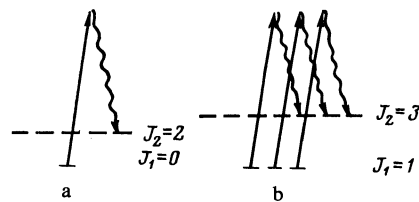

FIG. 1. Transitions between magnetic sublevels for CRS in parahydrogen, where $\Delta\omega = 354 \ \mathrm{cm}^{-1}$ (a), and in orthohydrogen, where $\Delta\omega = 587 \ \mathrm{cm}^{-1}$ (b).

We note also that the purely vibrational CRS in hydrogen, reported in Ref. 5, is due to the anisotropic part of the polarizability,[9,11] and therefore degeneracy in the projection of the total angular momentum is immaterial in this case.

2. THEORETICAL ANALYSIS

Consider rotational CRS excited by a step pulse. We express the exciting field $(\omega, k = \omega/c)$ and the scattered field $(\omega_s, k_s = \omega_s/c)$ in the form

$$\mathbf{E} = \frac{1}{2} \sum_{\sigma=-1,1} \mathbf{e}_\sigma \Big\{ \mathscr{E}_\sigma \exp[-i\omega t + ikz] + \mathscr{E}_\sigma{}^s \exp[-i\omega_s t + ik_s z] \Big\} + \text{c.c.}, \tag{1}$$

where $\mathbf{e}_\sigma$ is the vector of the field. In the course of the scattering the molecules undergo transitions between states with total angular momenta J_1 and J_2 and their projections M_1 and M_2. We shall omit hereafter the labels J_1 and J_2 and retain only the angular-momentum-projection labels M_1 and M_2. The equations for the amplitudes are

$$\frac{d}{dt} a_{M_1} = -\frac{i}{4\hbar} \sum_{\sigma,\sigma_1} (\alpha_{\sigma\sigma_1})_{M_1 M_2} \mathscr{E}_\sigma{}^s \mathscr{E}_{\sigma_1}{}^* a_{M_2},$$

$$\frac{d}{dt} a_{M_2} = -\frac{i}{4\hbar} \sum_{\sigma,\sigma_1} (\alpha_{\sigma\sigma_1})_{M_2 M_1} \mathscr{E}_\sigma{}^{s*} \mathscr{E}_{\sigma_1} a_{M_1}. \tag{2}$$

The matrix elements of the scattering tensor are given by the relation

$$(\alpha_{\sigma\sigma_1})_{M_1 M_2} = \frac{1}{\hbar} \sum_n \left[\frac{(d_{\sigma_1})_{M_1 n}(d_{-\sigma})_{n M_2}}{\omega_{n M_1} - \omega} + \frac{(d_{-\sigma})_{M_1 n}(d_{\sigma_1})_{n M_2}}{\omega_{n M_1} + \omega_s} \right],$$

where d_σ are the spherical components of the dipole moment.

Confining ourselves to the one-dimensional case in the given-exciting-field approximation, we supplement the system of equations (2) by an equation for the envelope of the scattering field

$$\frac{\partial}{\partial z} \mathscr{E}_\sigma{}^s + \frac{1}{c} \frac{\partial}{\partial t} \mathscr{E}_\sigma{}^s = 2\pi i k_s P_\sigma{}^s, \tag{3}$$

where the polarization $P_\sigma{}^s$ is given by

$$P_\sigma{}^s = \sum_{\sigma_1, M_1, M_2} (\alpha_{\sigma\sigma_1})_{M_2 M_1} a_{M_1} a_{M_2}{}^* \mathscr{E}_{\sigma_1}. \tag{4}$$

Before proceeding to the analysis of the nonlinear phase of the problem, we must determine the predominant polarization. This can be done within the framework of the linear approximation by comparing the growth rates of the different polarizations. The polarization with the faster growth will determine the nonlinear stage of the scattering.

In the nonlinear approximation the polarization $P_\sigma{}^s$ is given by

$$P_\sigma{}^s = \sum_{\sigma_1, M_1, M_2} (\alpha_{\sigma\sigma_1})_{M_2 M_1} \mathscr{E}_{\sigma_1}$$

$$\times \left[\rho_{M_1 M_2}(0) + \frac{i n_0}{4} \int_0^t dt' \sum_{\sigma_2, \sigma_3} (\alpha_{\sigma_2 \sigma_3})_{M_1 M_2} \mathscr{E}_{\sigma_1}{}^s \mathscr{E}_{\sigma_3}{}^* \right], \tag{5}$$

where

$$\rho_{M_1 M_2}(0) = a_{M_1}(0) a_{M_2}{}^*(0), \quad n_0 = |a_{M_1}(0)|^2 - |a_{M_2}(0)|^2.$$

The initial conditions, which reflect the specific features of the spontaneous triggering, are of the form

$$\rho_{M_1 M_2}(0) = \frac{i n_0 (\alpha_{\sigma\sigma_1})_{M_1 M_2}}{2 A_{\sigma\sigma_1}} \theta_0,$$

where

$$A_{\sigma\sigma_1}^2 = \sum_{M_1 M_2} |(\alpha_{\sigma\sigma_1})_{M_1 M_2}|^2. \tag{6}$$

The value of θ_0 must be chosen such that the scattering intensity be equal to the intensity of incoherent Raman scattering from the excited volume. If the Fresnel number for the scattering volume is equal to unity, an estimate yields[4]

$$\theta_0 \approx N^{-1/2}, \tag{7}$$

where N is the number of molecules in the excited volume. Relation (5) becomes particularly simple for linear and circular polarizations, for if the quantization axis is suitably chosen the subscripts $\sigma_{1,3}$ and σ_2 become identical. We introduce the notation

$$\theta = \theta_0 + \frac{A_{\sigma\sigma_1}}{2\hbar} \int_0^z dt' \mathscr{E}_{\sigma_1} \cdot \mathscr{E}_\sigma{}^s, \quad \tau = t - \frac{z}{c}. \tag{8}$$

In the linear case we have then for the function θ the equation

$$\partial^2\theta/\partial z \, \partial\tau = \beta\theta, \quad \beta = \pi k_s (2\hbar)^{-1} A_{\sigma\sigma_1} n_0 |\mathscr{E}_{\sigma_1}|^2. \tag{9}$$

For a rotator, such as the hydrogen molecule, there is a known explicit expression for the dependence of the scattering-tensor matrix elements on the rotational quantum numbers[9]; for the matrix element $A_{\sigma\sigma_1}$ we have (see the Appendix)

$$A_{\sigma\sigma_1}^2 = \frac{2}{75}(2J_1+1)(2J_2+1)\gamma_0^2 |\langle 1\sigma_1 1-\sigma | 2\sigma_1-\sigma\rangle \langle J_1 0 J_2 0 | 20\rangle|^2, \tag{10}$$

where γ_0 is the anisotropic polarizability.

Corresponding to the CRS problem are the following initial and boundary conditions:

$$\theta(z, \tau=0) = \theta_0, \quad -\frac{\partial}{\partial\tau}\theta(z=0, \tau) = 0. \tag{11}$$

The first corresponds to specifying on the exciting-pulse front an initial polarization that imitates spontaneous Raman scattering, while the second means that at the entry boundary of the medium there is no field having the scattering frequency.

Conditions (11) are satisfied by the solution 4

$$\theta = \theta_0 I_0(\eta), \quad \eta = 2(\beta z \tau)^{1/2},$$

where I_0 is a modified Bessel function of the first kind and of zero order. At large values of the argument

$$I_0(\eta) \approx (2\pi\eta)^{-1/2} e^\eta. \tag{12}$$

The growth rates of the function θ in time and in space are proportional to the parameter β. Using relations (9) and (10) we can determine the predominant polarization in the scattering. Thus, in the case of circular polarization of the exciting field the ratio of the growth rates for coinciding and opposing circular polarizations of the scattering field is 1:6. In

the case of linear polarization of the exciting field, the ratio of the growth rates for coinciding and orthogonal polarizations is 4:3.

We turn now to the essentially nonlinear problem. Let the exciting field have a circular polarization $\sigma_1 = 1$. In accord with the foregoing, the scattering field will then have the opposite circular polarization $\sigma = -1$, and the coinciding polarization can be neglected since it is exponentially small. The system of equations (2) breaks up then into $2J + 1$ two-level subsystems (see Fig. 1), where J is the smaller of the values J_1 and J_2. The solution takes in this case the form

$$a_{M_1} = a_{M_1}(0) \cos\left[\mu(M_1, M_2)\theta/2\right];$$

$$a_{M_2} = a_{M_1}(0) \sin\left[\mu(M_1, M_2)\theta/2\right], \tag{13}$$

$$\mu(M_1, M_2) = (\alpha_{1-1})_{M_1 M_2}/A_{1,-1}.$$

From (3), (4), and (13) follows an equation for the envelope of the scattering field:

$$\frac{\partial^2 \theta}{\partial z \, \partial \tau} = \beta \sum_{M_1, M_2} \mu(M_1, M_2) \sin[\mu(M_1, M_2)\theta]. \tag{14}$$

Using the explicit expression (A.1) and (A.2) for the matrix elements of the polarizability tensor at $J_1 = 1$ and $J_2 = 3$, we get

$$\mu(1, 3) = (5/7)^{1/2}, \quad \mu(0, 2) = (5/21)^{1/2}, \quad \mu(-1, 1) = (1/21)^{1/2},$$

$$\beta = {}^{3}/_{25}\pi k_s n_0 \hbar^{-1} \gamma_0^2 |\mathscr{E}_1|^2. \tag{15}$$

The linearized equation (14) reduces to Eq. (9). On the basis of the solution (12) we can estimate the characteristic times of the avalanche-like transitions between the sublevels. Clearly, an avalanche-like transition of particles between sublevels M_1 and M_2 occurs at the instant of maximum polarization at this transition, i.e., at

$$\mu(M_1, M_2)\theta = \pi/2. \tag{16}$$

Using the linear solution (12) and the condition (16), we estimate the delay times and the characteristic durations of the avalanches

$$t_0(M_1, M_2) \approx {}^{1}/_{4}\tau_0(M_1, M_2) \ln\left[\theta_0 \mu(M_1, M_2)\right]^{-1},$$

$$\tau_0(M_1, M_2) \approx \frac{1}{\beta z} \ln[\theta_0 \mu(M_1, M_2)]^{-1}. \tag{17}$$

It follows from (15) and (17) that the avalanche durations differ little, and the difference between the delay times is of the order of the avalanche durations. This can smooth out the temporal intensity pulsations that are features of the CRS in an extended medium.

Equation (14) was solved for the nonlinear case numerically. The solution of (14) for the coefficients given by (15) is shown in Fig. 2. At the parameter values indicated in Fig. 2 we get from (17) the relation $t_0 = 5\tau_0$ between the delay time and the duration of the first spike, in good agreement with the results of the numerical solution. By way of comparison, Fig. 3 shows the numerical solution of (14) in the absence of degeneracy. It can be seen from Figs. 2a and 3 that the dimensionless delay times are close to one another. Since the τ_0 time scale in Fig. 2 is inversely proportional to the field
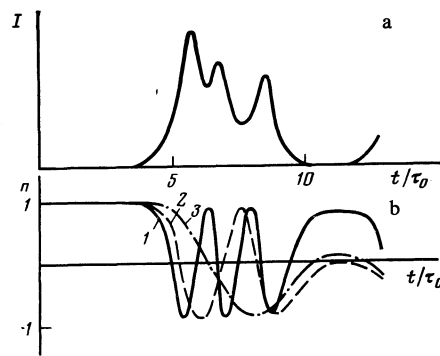

FIG. 2. a—Calculated shape of CRS pulse in orthohydrogen b—time dependence of the population difference between the magnetic sublevels. $1 - M_1 = 1 \rightarrow M_2 = 3$, $2 - M_1 = 0 \rightarrow M_2 = 2$, $3 - M_1 = -1 \rightarrow M_2 = 1$, $\lambda_s = 1.128$ μm, $\tau_0 = 2.9$ nsec, $n_0 = 0.45$ cm^{-2}, $l = 10$ cm, $\tau_0 = (\beta z)^{-1} \ln \theta_0^{-1}$.

growth rate, to which all the transitions contribute, equality of the delays means that the level degeneracy does not affect the temporal properties of the CRS within times up to the maximum of the first spike. At times longer than the delay times, the differences between the pulse shapes are quite substantial.

As seen from Fig. 2b, avalanche-like transitions of molecules for different sublevel pairs are shifted in time, and the oscillations have different frequencies, as is manifest by the smoothening of the scattering-intensity pulsations compared with a purely two-level transition. The intensity pulsations in a degenerate system have a noticeably shorter period then in a two-level system. The times of the maxima of the scattering intensity are close to those of the minima of the population difference of the strongest transition $M_1 = 1 \rightarrow M_2 = 3$ (curve 1 of Fig. 2b). This is a distinguishing feature of a two-level system.[2]

The decrease of the period of the intensity pulsation and the corresponding increase of the population oscillation frequency can be apparently attributed to the smearing of the temporal structure of the scattering pulse. It can be seen from Figs. 2a and 2b that in the interval $t/\tau_0 < 10$, where the field does not drop to zero, the sublevel populations move faster than on the interval $t/\tau_0 > 10$, when the nonlinear synchronization of the transition causes the field to drop to zero. The population motion is noticeably showed down in the latter case.

It should be note that equations similar to (14) were considered in a number of papers devoted to the theory of self induced transparency in degenerate systems (a bibliography can be fond in the review 12). It was established that stationary $2\pi n$ pulses exist only at integer ratios of the coeffi-
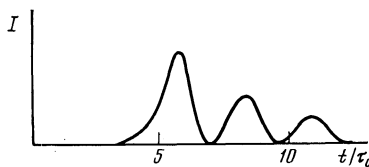

FIG. 3. Calculated shape of CRS pulse in orthohydrogen. $n_0 = 1.1 \times 10^{19}$ cm^{-3}, $l = 10$ cm, $\lambda_s = 1.097$ μm, $\tau_0 = 1.9$ nsec, $\tau_0 = (\beta z)^{-1} \ln \theta_0^{-1}$.

cients $\mu(M_1, M_2)$. In the general case, however, the desynchronization of the different transitions makes existence of stationary pulses impossible. This difference in the manifestation of the level degeneracy in self-induced transparency phenomena and in cooperative radiative processes is in full analogy with the onset of transverse spatial inhomogeneity of the field. In the latter case, desynchronization of the transitions of atoms located at different distances from the beam axis also leads not to be presence of stationary pulses in self-induced-transparency phenomena, but only to a smoothing of the temporal structure of the radiation in cooperative radiative processes.

3. EXPERIMENTAL SETUP

We used in the experiments a phosphate glass + neodymium laser system operating at a wavelength $\lambda = 1.056$ μm. A diagram of the setup is shown in Fig. 4. The emission spectrum of laser 1 consisted of one TEM_{00q} mode, and the spectrum width did not exceed 2×10^{-3} cm^{-1}. The leading front of the laser pulse was shortened to 1–4 nsec by the electronic shutter 2. The shutter was actuated by a laser-ignited discharge at an instant corresponding to the maximum laser-pulse intensity. After passage through the amplifiers 3 and 6 the laser pulse had an energy $W_L = 0.75$ J at a duration $t_L = 100$ nsec or $W_L \leqslant 0.5$ J at $t_L = 30$ nsec. The Fresnel biprism 5, placed between the amplifier stages, transformed the laser-emission polarization from linear to circular and served, together with the Glan prism 4, to decouple optically the laser, on the one hand, from the amplifier and the cell 8 with hydrogen, on the other.

The laser radiation was focused into the hydrogen-filled cell by a lens whose focal length F ranged from 40 to 85 cm. Three cells 8.5, 30, and 90 cm long were used. The cell windows were tilted 5° to prevent feedback. Variation of the cell length in the course of the experiment has made it possible to establish that the effective length l of the scattering volume coresponds to two confocal parameters of the focused beam $l = 2b = 2kr_0^2$, where r_0 is the radius of the beam neck at the $1/e$ level. The main experiments were performed with an $F = 61$ cm lens and a 90-cm cell. In this case the area of the spot in the focal plane, at the $1/e$ level, was 3×10^{-4} cm^2, and the effective length was $l \approx 10$ cm.
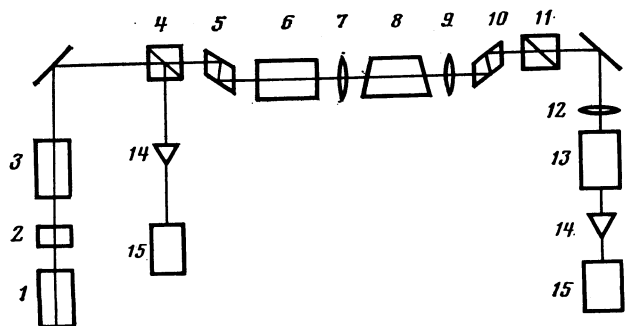

FIG. 4. Diagram of experimental setup: 1— neodymium laser; 2—electronic shutter; 3, 6—amplifier system; 4, 11—Glan prisms; 5, 10—Fresnel biprisims; 7, 9, 12—lenses; 8—cell with hydrogen; 13—monochromator; 14—coaxial photocells, 15—oscilloscopes.

The polarization of the radiation emerging from the hydrogen cell was analyzed with the Fresnel biprism 10 and the Glan prism 11. The scattered radiation was separated by monochromator 13 having a dispersion 20 Å/mm. The waveforms of the laser and scattered-radiation pulses were recorded with FÉK-15 coaxial photocells and I2-7 oscilloscope. The temporal resolution of the recording system was 1 nsec (at half maximum), and the triggering stability, which determines the accuracy of the time-delay measurement, was also close to 1 nsec.

4. EXPERIMENTAL RESULTS AND THEIR DISCUSSION

Natural hydrogen is a mixture of 25% parahydrogen and 75% orthohydrogen. In this mixture the CRS observed at room temperature is from the orthohydrogen (the S_0 (1) line). To obtain CRS from parahydrogen (the S_0 (0) line) its content was increased to more than 90%. The enrichment was by adsorption of hydrogen on the surface of activated carbon cooled with liquid helium.[13]

Figure 5 shows oscillograms of the pulses of rotational CRS in para- and orthohydrogen. The oscillograms were obtained under near-threshold conditions, at a scattering power less than 10% of the laser power, i.e., the given-exciting-field approximation was valid. The scattering pulses in parahydrogen (Figs. 5b–f) are characterized by a delay and by temporal pulsations, common features of cooperative processes in an extended medium. The CRS pulses in orthohydrogen are also shifted in time, but their envelope is smooth and shows no pulsations (Fig. 5g).

Let us discuss certain additional experimental facts of importance for the interpretation of the oscillograms of Fig. 5. Under all experimental conditions the CRS polarization was circular and directed opposite to the polarization of the exciting radiation, in agreement with the discussion in Sec. 2. Scattering by both ortho- and parahydrogen was only in laser-pulse propagation direction. No radiation in the opposite direction was observed at a recording-system sensitivity 2×10^{-4} J. Photography of the intensity distributions of the laser and scattered radiation near the focal plane of the

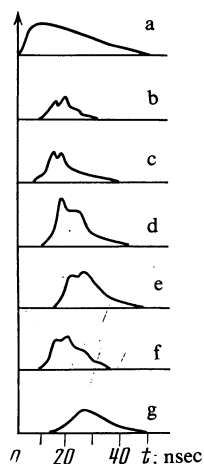FIG. 5. Oscillograms of laser pulse (a) and CRS pulses in parahydrogen (b–f) and orthohydrogen (g), $W_L - 0.26$ J, $T = 300$ K, $p = 1.1$ atm (b–d); $T = 170$ K, $p = 0.36$ atm (e, f); $T = 300$ K, $p = 0.7$ atm (g).

$F = 61$ cm lens showed that no self-focusing of the radiation in the hydrogen occurs under the conditions of our experiment. The scattered radiation was concentrated into a single spot. The CRS divergence was close to that of the laser emission.

In the investigated pressure region $p \leqslant 6$ atm the scattering spectrum consisted of only the first Stokes line of the rotational CRS. At a recording sensitivity 3×10^{-3} J, we observed no anti-Stokes rotational scattering, nor vibrational CRS, nor high-power pulses for Stokes lines of higher order. The experimental regime thus satisfied the main conditions assumed in the theoretical analysis in Sec. 2. Namely, the scattering was unidirectional; its spectrum contained only one component; the CRS polarization was circular and opposite; there was no attenuation of the exciting field. The observed pulsations can therefore not be due to the causes previously discussed in the literature, viz., interaction of Stokes and anti-Stokes waves[5] and attenuation of the exciting field.[14]

We discuss first the shape of the CRS pulse in parahydrogen. Oscillograms 5b–5d were obtained at a pressure $p = 1.1$ atm and at room temperature (population difference $n_0 = 1.1 \times 10^{19}$ cm^{-3}). Under these conditions the measured delay time of the first pulse is $t_0 = 10 \pm 3$ nsec, and the pulsation period is from 3 to 6 nsec. The CRS pulses with longer pulsation periods had a longer delay, Let us compare the measured values with the theory. The time scale for Fig. 3 can be calculated from Eqs. (17). Using relations (7), (8), and (17), assuming $\gamma_0 = 0.31 \times 10^{-24}$ cm^3 (Ref. 11), and putting $\mu(M_1, M_2) = 1$ we get

$$\tau_0 = ({}^1/_{15}\pi k_s \hbar^{-1} n_0 \gamma_0^2 l |\mathscr{E}_1|^2)^{-1} \ln (1/\theta_0).$$

Under the conditions corresponding to the oscillograms 5b–5d ($I_L = 10^{10}$ W/cm^2, $l = 10$ cm, $n_0 = 1.1 \times 10^{19}$ cm^{-3}) we get $\tau_0 = 1.9 \times 10^{-9}$ sec. Bearing the given time scale in mind, we conclude from Fig. 3 that the calculated pulsation periods 4.5 nsec and the delay time $t_0 = 9.5$ nsec agree well with the measured values. The depth of the CRS intensity pulsations observed in experiment, however, is much smaller than that calculated in the one-dimensional model of Fig. 3. Approximately half the CRS pulses had no pronounced temporal structure.

The smearing of the structure may be due to relaxation of the polarization.[15] It follows from the measured spontaneous RS line width[16] that the polarization relaxation time for the $S_0(0)$ line at $p = 1.1$ atm is $T_2 \gtrsim 3$ nsec. It is possible to increase T_2 within certain limits by cooling the gas. With decreasing temperature the parahydrogen molecules go over from the level $J_2 = 2$ to the ground level $J_1 = 0$, i.e., a specified population difference can be achieved at a lower total density of the gas. Corresponding to the lower density is a longer relaxation time. Figures 5e and 5f show oscillograms obtained when the cell with the hydrogen was cooled to 170 K. The gas pressure in this case was $p = 0.36$ atm and the population difference was $n_0 = 1 \times 10^{19}$ cm^{-3}. It can be seen that the pulsation depth did not decrease.

It appears that the main reason why the CRS intensity does not decrease to zero between spikes is that the scattering volume constitutes in our case the neck of a focused Gaussian beam. As shown in Refs. 6 and 7, a transverse inhomogeneity of this type led to partial smoothing of the temporal structure.

The CRS pulse shape in parahydrogen varies appreciably from flash to flash. In particular, in a number of flashes we observed CRS pulses in which the first spike had the largest amplitude (Figs. 5c, d). At the same time, we recorded pulses in which the first spike was not the largest (Figs. 5b, e, f).

It must be noted that within the framework of the one-dimensional theory the first spike in a cooperative-emission pulse is always the largest. In a number of cases, however, the transverse inhomogeneity leads to a redistribution of the radiation energy among the spikes.[6,7] The fluctuations of the different triggerings cause the pulse shape to be substantially nonuniform in the three-dimensional case.[6] The numerical calculations of Ref. 6, in which these factors were taken into account, have shown that the variations of the cooperative-emission pulse shape to be as large and of the same character as those shown in Figs. 5b–f.

We proceed now to a discussion of scattering in ortho-hydrogen. The pulse oscillogram shown in Fig. 5g was obtained for the same laser-pulse parameters, focusing conditions, and approximately the same relaxation time $T_2 = 4$ nsec as in the case of parahydrogen (Figs. 5b–d). Under the conditions indicated in Fig. 5, the parameter β, which determines the characteristic times of the CRS pulses, is one and one-half times larger for ortho- than for parahydrogen. Under the conditions indicated, the power of the CRS pulses in orthohydrogen fluctuates considerably, the duration at half maximum ranges from 10 to 15 nsec, but no pulsations are observed in any of the recorded pulses. The pulse shape remained smooth up to $p = 0.4$ atm ($T = 300$ K) when the relaxation time was increased to $T_2 = 5$ nsec. Since the geometric factors that the determine the role of the transverse effects are also the same for scattering in ortho- and parahydrogen, there is every reason to attribute the differences between the CRS pulse shapes in these cases to the difference in the degree of energy-level degeneracy.

Calculation of the CRS pulse shape in orthohydrogen for the one-dimensional model and $T_2 = \infty$ (Fig. 2a) shows that level degeneracy leads to a noticeable decrease of the pulsation depth. The joint action of degeneracy effects and transverse effects leads to the complete CRS-pulsation smoothing observed in the experiments. The time scale calculated from Eqs. (15) and (17) for Fig. 2 is $\tau_0 = 2.9$ nsec. The calculated delay time $t_0 = 14.5$ nsec (see Fig. 2) is thus in satisfactory agreement with the measured value 19 ± 5 nsec.

The results described were obtained in the subthreshold regime, when the coefficient of conversion into the Stokes component is small. When the hydrogen pressure is raised above threshold, the power and duration of the CRS pulse increase considerably, and the energy of the Stokes scattering reaches 70% of the laser-pulse energy. In the laser-field damping regime, the CRS pulse in orthohydrogen remained smooth, while for parahydrogen pulsations were observed in the intensities of both the CRS and of the exciting radiation passing through the hydrogen.
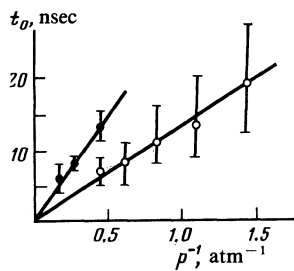
FIG. 6. Rotational CRS delay time in orthohydrogen vs gas pressure and laser pulse energy, $t_L = 100$ nsec; ●—$W_L = 0.45$ J, ○—$W_L = 0.75$ J.

Irradiation of a mixture with approximately equal ortho- and parahydrogen contents produced CRS from both modifications, with pulsations on the pulses of both the CRS and the passing laser radiation. The CRS pulsations in orthohydrogen are due in this case to the laser-emission pulsations caused by the interaction with the parahydrogen.

We note in conclusion a number of facts that are of importance in the interpretation of the experimental results. The delay time t_0 is inversely proportional to the hydrogen pressure and to the laser-emission intensity. Figure 6 shows plots of the delay time of the CRS from the $S_0(1)$ line on the hydrogen pressure of two laser-pulse energies and at equal duration t_L. The plot shows a maximum scatter of t_0 in five–six pulses at $W_L = 0.75$ J and three–four pulses at $W_L = 0.45$ J. The experimentally obtained relation $t_0 \sim p^{-1} W_L^{-1}$ agrees with the CRS theory [see Eqs. (15) and (17)].

The delay time decreases with increasing duration of the leading front and of the width of the exciting-radiation spectrum. This is evidence that the delay is due to the coherent character of the interaction between the radiation and the medium.

The experiments have shown that at the cited hydrogen pressures and laser power the delay time remains constant when the focal length F of the lens ranges from 40 to 85 cm. The reason is that the CRS delay time depends on the product of the exciting-field intensity by the length of the scattering volume [see (15) and (17)]. For a Gaussian beam the length is $l \propto r_0^2 \propto F^2$ and the intensity is $I_L \propto r_0^{-2} \propto F^{-2}$, meaning that t_0 should not depend on F.

It follows from the CRS energy measurements that a significant redistribution of the populations of the H_2 levels is produced by the scattering. This is also a distinguishing feature of a cooperative process. Thus, near the CRS threshold the number of photons in the scattering pulse is $N_s = W_s/\hbar\omega_s = 10^{17}$, and the number of orthohydrogen molecules in the state $J_1 = 1$ in the volume bounded by the laser-beam neck is $N = n_0\pi r_0^2 l \approx 6.10^{16}$.

CONCLUSION

The experiments have shown that in the case of coherent nonstationary excitation a rotational Raman scattering pulse in parahydrogen has all the characteristic features of a cooperative process, viz., delay relative to the excitation front, pulsations of the intensity, and a delay time inversely proportional to the gas density and to the laser intensity. The

pulse is accompanied by an appreciable change of the populations of the combining levels.

The measured delay times and pulsation period of CRS in parahydrogen are in good agreement with the calculated ones. The shape of the CRS pulse in parahydrogen fluctuates considerably; this may be due to the joint effect of the finite excitation aperture, and hence of the transverse inhomogeneity of the scattering field, on the one hand, and the fluctuations of the spontaneous triggerings, on the other.

A comparative experimental investigation of the rotational CRS pulse shape has shown that, in contrast to scattering in parahydrogen, the envelope of the CRS pulse in orthohydrogen is smooth. We attribute this difference to the fact that the CRS in orthohydrogen is due to transitions between three pairs of magnetic sublevels. A theoretical analysis and numerical calculations within the framework of the one-dimensional model have revealed the following features of the cooperative process in a degenerate system: Avalanche-like transitions in different sublevel pairs are not in synchronism, and this manifests itself in a substantial decrease of the depth of the radiation-intensity pulsations. The period of the intensity pulsations is smaller in a degenerate system than in a two-level system.

The degeneracy of the energy levels is thus a significant physical factor that must be taken into consideration in the analysis of cooperative processes, particularly of the cooperative scattering and emission pulse shape.

APPENDIX

The matrix elements of the scattering tensor of a rotator have an explicit dependence on the rotational quantum numbers[9]:

$$(\alpha_{\varkappa q})_{M_2 M_1} = \frac{1}{5}[(2J_1+1)(2J_2+1)]^{1/2}\bar{\alpha}_{20}\delta_{\varkappa 2}i^{J_1+J_2}(-1)^{J_2-M_2}$$
$$\times\langle J_1-M_1 J_2 M_2|2-q\rangle\langle J_1 0 J_2 0|20\rangle, \qquad (A.1)$$

where $\bar{\alpha}_{20}$ is a component of the irreducible tensor in a coordinate frame rigidly connected with the molecule. This component can be expressed in terms of the anisotropic polarizability γ_0 in the form $\bar{\alpha}_{20} = (\frac{2}{3})^{1/2}\gamma_0$.

We use the following representation for the irreducible tensor operators[17]

$$(\alpha_{\sigma\sigma_1})_{M_2 M_1} = \sum_{\varkappa,q}\langle 1\sigma_1 1-\sigma|\varkappa q\rangle(\alpha_{\varkappa q})_{M_2 M_1}. \qquad (A.2)$$

Substituting (A.2) and (A.1) in (6) and taking into account the orthogonality of the Clebsch-Gordan coefficients, we obtain Eq. (10).

[1] N. Skribanowitz, I. P. Herman, J. C. McGillivray, and M. S. Feld, Phys. Rev. Lett. **30**, 309 (1973).
[2] J. C. McGillivray and M. S. Feld, Phys. Rev. **A14**, 1169 (1976).
[3] H. M. Gibbs, Q. H. F. Urehen, and H. M. Hikspoors, Phys. Rev. Lett. **39**, 547 (1977).
[4] B. M. Chernobrod, Opt. Spektrosk. **49**, 692 (1980).
[5] V. S. Pivtsov, S. G. Rautian, V. P. Safonov, K. G. Folin, and B. M. Chernobrod, Zh. Eksp. Teor. Fiz. **81**, 468 (181) [Sov. Phys. JETP **54**, 250 (1981)].
[6] E. A. Watson, F. P. Mattar, H. M. Gibbs, M. Cormier, Y. Claude, S. I. McCall, and M. S. Feld, Phys. Rev. **A27**, 1427 (1983).
[7] F. P. Mattar and C. M. Bowden, Phys. Rev. **A27**, 345 (1983).

[8]S. G. Rautian, V. P. Safonov, and G. B. Chernobrod, Pis'ma Zh. Eksp. Teor. Fiz. **35**, 144 (1982) [JETP Lett. **35**, 174 (1982)].

[9]V. B. Berestetskii, E. M. Lifshitz, and L. P. Pitaevskii, Relativistic Quantum Theory, Part 1, Pergamon, 1971, Chap. VI.

[10]Yu. A. Il'inskii and V. D. Tarnukhin, Kvant. Elektron. (Moscow) **1**, 401 (1974) [Sov. J. Quant. Electron. **4**, 224 (1974)].

[11]W. Kolos and L. Woniewicz, J. Chem. Phys. **46**, 468 (1967).

[12]I. A. Poluektov, Yu. M. Popov, and V. S. Roïtberg, Usp. Fiz. Nauk **114**, 97 (1974) [Sov. Phys. Usp. **17**, 673 (1975)].

[13]A. Farkas, Orthohydrogen, Parahydrogen, and Heavy Hydrogen, [Russian transl.] M.-L, ONTI, 1936.

[14]G. I. Kachen and W. H. Lowdermilk, Phys. Rev. **A14**, 1472 (1976).

[15]N. I. Shamrov, Abstracts, 2nd All-Union Symp. on Optical Echo, Kazan', 1981, p. 108.

[16]W. G. Cooper, A. D. May, E. H. Hara, and H. F. P. Knapp, Can. J. Phys. **46**, 2019 (1968).

[17]D. A. Varshalovich, A. N. Moskalev, and V. K. Khersonskii, Kvantovaya Teoriya uglovogo momenta (Quantum Theory of Angular Momentum), Nauka, 1975.

Translated by J. G. Adashko